Journal of
Mechanical
Science and
Technology

Journal of Mechanical Science and Technology 21 (2007) 1253~1262

Application of Temperature-Sensitive Paint for Surface Temperature Measurement in Heat Transfer Enhancement Applications

Joosung J. Lee[a,*], J. Craig Dutton[b], Anthony M. Jacobi[c]

[a]*Department of Industrial and Information Engineering, Yonsei University, Seoul 120-749, Korea*
[b]*Department of Mechanical and Aerospace Engineering, University of Texas at Arlington, Arlington, Texas 76019-2906, USA*
[c]*Department of Mechanical Science and Engineering, University of Illinois at Urbana-Champaign Urbana, Illinois 61801-0018, USA*

(Manuscript Received October 9, 2006; Revised May 10, 2007; Accepted May 11, 2007)

Abstract

This paper introduces the use of temperature-sensitive paint (TSP) to obtain the whole-field temperature distributions in heat transfer enhancement applications. Knowing the surface temperatures in such applications is important to quantify the heat transfer, as well as to obtain insight into the flow physics. Applying the TSP to a flat plate with and without a vortex generator showed that the TSP Nusselt number distribution over the flat plate alone matched the Blasius solution with less than 10% error. The TSP temperature distribution of the flat plate with the delta wing vortex generator showed a local heat transfer enhancement of about 30% and the locations of temperature extremes. This paper also provides a detailed guideline for the application, image acquisition, and image processing procedures for TSP along with its calibration surfaces.

Keywords: Temperature-sensitive paint; Surface temperature measurement; Vortex generator; Heat transfer enhancement

1. Introduction

In many heat transfer enhancement systems, such as for air conditioning and refrigeration (AC/R) applications, surface temperature variations of the system components can be large. Moreover, the locations of surface temperature extremes can coincide with thermally and mechanically stressed areas, in which case a sudden failure might occur. Consequently, understanding surface temperature distributions is crucial in heat transfer augmentation applications, as it also provides insight into the flow and heat transfer interactions. However, conventional methods of measuring surface temperatures, such as thermocouples, thermistors, or resistance temperature detectors (RTDs), are intrusive point measurements and can miss the locations of extremes when temperature variations are large. Therefore, a non-intrusive full-field method is required to determine accurate surface temperature distributions of complex heat transfer enhancement systems.

In this work, temperature-sensitive paint (TSP) is employed to obtain the full-field temperature distributions of flat plate-vortex generator surfaces. Further development and assessment of the method for heat transfer enhancement applications are also required, since there is little experience with the TSP method. This is despite the fact that TSP has advantages in that it is an inexpensive method for obtaining full-field temperature distributions in a non-intrusive manner. Image acquisition, data reduction, surface calibration, and reduction of the noise signal are also discussed.

*Corresponding author. Tel.: +82 2 2123 5724, Fax.: +82 2 364 7807
E-mail address: JSL@yonsei.ac.kr

2. Background

Fluorescence is the process by which molecules of a substance are excited by absorbing light and then transition back to the original ground state as they emit the absorbed light in the form of photons of a longer wavelength. The TSP method utilizes this fluorescence process of organic luminophores suspended in a polymeric binder. If the binder holding the luminescent probe molecules is oxygen-impermeable, the rate of fluorescence emission is dominated by temperature effects, as temperature-dependent non-radiative deactivation becomes the primary source of fluorescence suppression. As a result, the intensity of TSP fluorescence is inversely proportional to temperature as shown in Eq. (1).

$$\ln\left(\frac{I(T_{ref})}{I(T)}\right) = -\frac{E_a}{R}\left(\frac{1}{T} - \frac{1}{T_{ref}}\right) \quad (1)$$

where (E_a/R) is the activation energy. This relation is obtained by assuming that the fluorescence intensity of TSP at 0 K is much greater than at ambient temperature (Liu and Sullivan, 2004).

3. Experimental facilities and instrumentation

3.1 Temperature-sensitive coatings

The TSP used in this experiment is from the School of Aeronautics and Astronautics at Purdue University (PUR TSP). The PUR TSP consists of 0.1 g of Ru (bpy) (2,2'-bipyridine ruthenous dichloride hexahydrate, GFS Chemicals item number 114) mixed with 35 ml of Zinsser Bull's Eye Shellac (Campbell et al., 1998). Various types of temperature-sensitive paint luminescent molecules for other applications can be found in Liu *et al.* (1997). Also, different polymer binders can be selected according to the temperature range of the experiment. For example, using Ru (bpy) in airplane dope as a binder makes it possible for the temperature range of TSP to be extended up to 100 °C (Liu *et al.*, 1997).

A Badger 250 external-mixing airbrush was used for applying the TSP to the surface, while air was supplied by a Campbell Hausfeld PowerPal MT 5001 air compressor. Spraying TSP requires careful preparations and some experience in order to produce a smooth and uniform surface. First, the surface to be painted is roughened with 400 A sandpaper and cleaned with ethanol. The extra surfaces that need not be painted are then masked off, before a first layer of white primer (Zinsser item number 1008) is applied to the surface. After thirty minutes, a second layer of the primer coating is applied. Up to eight hours may be required for the primer surface to dry completely. The primer surface is then roughened with 600 A sandpaper to remove any large particles or irregularities.

The application of TSP is done in a similar manner as for the primer, but cleanliness is of utmost importance at this stage, because any dust particles or scratches will become the sources of noise in the TSP intensity data. Since the shellac does not immediately flow onto the primer surface and tends to form streaks, a very small amount should be continuously applied with a repetitive motion until a relatively thick and uniform coating is obtained. It takes about another eight hours for the TSP to dry. Slightly heating the dry TSP surface with any source of moderate heat, such as a hair dryer or thermal chamber, then helps re-flow the shellac and achieve an even smoother and more uniform TSP coating.

Once the TSP is applied, touching or excessively exposing the painted surface to the atmosphere should be avoided to keep the TSP surface clean and intact. The TSP surface is soft initially, but it becomes hardened as it dries over time. Thus, it is necessary to apply a fresh TSP coating on the specimen about every two weeks. Since fabrication of a completely new specimen for each set of measurements is not economical in many cases, the original TSP coating can be thinned by using ethanol or shellac thinner. This also helps smooth out surface variations in the previous TSP coating. Then a new batch of TSP can be applied on top of the old, thinned TSP surface.

There are two types of optical filters used in imaging the TSP surface, one excitation filter and one emission filter. To illuminate the TSP surface, an excitation band-pass filter with a wavelength range of 450 ± 10 nm (Melles Griot 03FIV028) is placed on top of a specially-fabricated light source with a 75 W tungsten-halogen bulb. The emission band-pass filter with a wavelength range of 600 ± 10 nm (Melles Griot 03FIB014), used to detect the emission from the TSP surface, is placed on the camera lens (Nikon 55 mm f/2.8) by means of a modified standard filter holder.

A Photometrics CH250 CCD camera (14 bit, unintensified, 512 × 512 Tektronix array, pixel size $(23\ \mu m)^2$) is used to record the TSP fluorescence. It consists of the following units: camera head, shutter

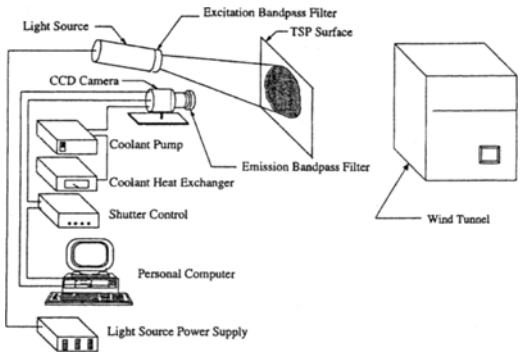

Fig. 1. Schematic of experimental setup. (modified from Woodmansee, 1997)

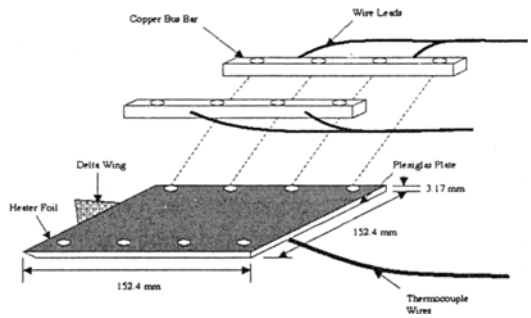

Fig. 2. Schematic of flat plate-vortex generator geometry.

controller, and cooling unit. A ZEOS 486 PC, together with Photometrics PMIS software, was used to drive the CCD camera system for imaging the TSP surfaces. This experimental setup is shown in Fig. 1.

3.2 Flat plate-vortex generator and wind tunnel system

The flat plate-vortex generator system of Gentry (1998) in Fig. 2 is the experimental geometry for testing the TSP. It consists of a flat plate with a vortex generator mounted at the leading edge, a wind tunnel test section where the plate is placed horizontally with the top (heated) side facing down, an electrical power supply, and a wind tunnel system. The top side of the plate is covered with a sheet of metal foil, which is heated by the electrical power supply through a pair of copper bus bars. The temperature-sensitive paint coating is applied on the top side of the heater foil to measure the surface temperature distribution as convection heat transfer occurs over the foil surface.

The plate (152.4 mm × 152.4 mm × 3.17 mm) is made of Plexiglas with low thermal and electrical conductivity, so that negligible conduction heat loss through the backside of the plate can be assumed. However, the conduction heat loss through the foil has been experimentally found to be as large as 5 % and is accounted for in the flat plate heat transfer energy balance. As a result, some extra insulation materials were placed on the backside of the plate for the purpose of minimizing the conduction heat loss. The plate is held in place by two slots grooved on both sides of the test section. The plate's leading edge has been ground at 18.4° to a sharp tip in order to minimize flow disturbances in the neighborhood of the tip.

Fecralloy (Goodfellow item number FE080250), an iron/chromium alloy (Fe72.6/Cr22/Al4.8/Si0.3/Y0.3) foil, with a thickness of only 0.05 mm and electrical resistivity of 134 μΩ-cm was selected for the heater foil. Note that a thin heater foil is required to minimize conduction through the thickness of the foil itself while maximizing convection from the surface. At the same time, the electrical resistance of the foil should be large so that the foil heats up easily with a small amount of applied electrical power. As a result of the nearly uniform electrical heating of the foil, a constant heat flux boundary condition is assumed in the flat plate heat transfer experiments of this work. In order to minimize the leading edge effect, the heater foil was firmly epoxied down on the Plexiglas plate along the leading edge. Heat-resistive grease was also applied between the rest of the foil and the plate surfaces to minimize contact resistance.

Omega type-T thermocouples are mounted on the foil to measure surface temperatures and to provide calibration data for the TSP method. Since attaching the thermocouples on the painted surface introduces disturbances to the flow, small holes were drilled on the back of the Plexiglas plate, and the thermocouples were placed on the backside of the foil. Good contact between the thermocouple and the foil is crucial to ensure accurate measurements of foil temperatures. In addition, it is desirable to locate thermocouples at the points of expected temperature extremes in order to obtain calibration data spread over a wide range of temperatures. Therefore, the thermocouples are mainly located along the streamwise direction, because the temperature gradients mainly occur in the flow direction in the experiments of this work. A LabView program is used for acquiring the thermocouple temperature measurements.

A pair of copper bus bars (152.4 mm × 9.52 mm × 3.17 mm) are used to provide uniform current through the foil. Each one is mounted on the plate by means of four flat-head screws and is slid into the slots in the test section walls. Silver paint is then applied along the junction of the bus bars and the foil surface to ensure good electrical contact and uniform electrical power dissipation through the foil. Two wire leads are attached with Allen-head screws to each bus bar from the outside of the wind tunnel test section to make connection to the electrical power supply.

A Hewlett Packard 6269B DC power supply provides a maximum current of 60 amps, while a proper range of operation is between 0 to 20 amps for the selected heater foil and the experimental setup. Current and voltage just across the foil are measured by a Fluke-27 multimeter.

The wind tunnel test section is made of Plexiglas. The complete wind tunnel system, manufactured by Engineering Laboratory Design Inc., has three major components, the inlet with a honeycomb flow straightener and a series of screens, the test section with an inlet-to-test section area contraction ratio of 9:1, and the outlet with an exhaust fan, an acoustic diffuser, and a mass flow meter.

The airflow passes through the contraction and flow straightener sections and has a spatially uniform, low freestream turbulence velocity profile. The measured turbulence intensity is between 0.95% and 1.25% for a test section mean velocity range of 0.68 to 2.58 m/s, and the maximum mean velocity non-uniformity is 3.16% for the approach velocity profile (De Jong and Jacobi, 2003; Gentry, 1998). For actual air speed measurements inside the test section, a TSI VelociCalc hot-ball anemometer was used. A typical inlet air temperature ranged between 18 to 20 °C, which was measured by a thermometer at the inlet.

4. Experimental procedure

4.1 Image acquisition

When the TSP-painted foil was ready and assembled with the flat plate-vortex generator attached, the TSP-painted surfaces were imaged in the following three conditions: heat-off/wind-off, heat-on/wind-off, and heat-on/wind-on. Since the TSP surface was installed facing down in order to minimize natural convection, obtaining images of such a surface requires careful lighting and camera setup underneath the wind tunnel test section. In addition, TSP image acquisition is conducted in a completely dark room with only the TSP light source on in order to eliminate noise from any unnecessary lighting and to obtain the best TSP surface response possible.

Focusing is one of the most important steps in TSP image acquisition. Since it is difficult to focus on the bare TSP surface, a piece of white paper with some small letters in black ink was placed on top of the TSP surface as an object of focus. Note that focusing is done under the coldest condition of the expected experimental temperature range (usually no-heat/no-wind condition), because the TSP intensity will otherwise further increase beyond the range of the CCD camera if, during the experiment, temperatures should drop below that at the time of focusing.

Lighting is another important aspect of image acquisition because it can be a major source of noise if it is not properly located. It is most ideal to illuminate the TSP surface of interest evenly. Therefore diffusing paper was placed on the front of the light source. In addition, the light source was placed at an angle, about 3 feet away from the TSP surface so that direct reflection of the light bulb did not cause any glare in the TSP surface images; see Fig. 1.

Once all preliminary work was complete, TSP images in the three conditions described above were acquired in the temperature range of 20 to 50°C. As another method of reducing noise signals, 20 images were obtained for each condition and averaged. First, a reference image, which is used for normalization, was obtained at a reference temperature. This is usually the no-heat/no-wind condition in which the TSP intensity is at its highest level. Second, a dark image was also acquired to account for camera noise and was subtracted from all other images obtained with the CCD camera. Third, for static calibration purposes, a series of heat-on/wind-off images was acquired as the electrical power supplied to the foil heater was increased gradually with a current increment of 1A.

Heat-on/wind-on conditions are the primary experiments of interest for AC/R applications. In this work, flat plate images with and without a delta wing vortex generator have been obtained to emphasize application of TSP in heat transfer augmentation applications. For each experiment, a new reference image was obtained, and then the experimental images were acquired. After this, the whole-field

surface temperature distributions were determined by *in-situ* calibration. It is extremely important that there should be no pixel shift in all images obtained for each experiment because any spatial misalignment between the reference image and the run images results in a large noise component in the normalized image.

As the TSP images were being acquired, the corresponding thermocouple temperature measurements were also made. The temperatures were continuously acquired and averaged over the period of the image acquisition for each experiment.

In order to calculate the power dissipation just across the heater foil surface, voltage and current measurements were made for each experiment. Especially, voltage drop was carefully measured across the farthest ends of the foil in the spanwise direction to determine the most accurate power dissipation possible of the heater foil. In addition, the freestream wind speed was measured inside the wind tunnel test section by the hot ball anemometer.

4.2 Image processing

Once image acquisition was complete, the obtained images were further processed in order to obtain a calibration curve and the full-field surface temperature distributions. Since 20 images were acquired for each experimental condition, they were averaged by a FORTRAN program.

The normalization of the images then follows the averaging process. The purpose of normalization is to account for non-uniformity in the TSP images due to uneven lighting, variations in the TSP coating, camera noise, and non-uniform response of the camera pixels. In addition, the normalization scheme enables the user to analyze the data in a non-dimensional form; therefore, the change in intensity appears as the change in the ratio of the intensity of the reference condition to the intensity of a certain experimental condition as shown in Eq. (2).

$$\text{IR (Intensity Ratio)} = (I_{ref} - I_{dark}) / (I_{run} - I_{dark}) \qquad (2)$$

Subscripts ref, run, and dark denote reference condition, run condition, and dark image, respectively. Note that the dark image is subtracted from all the images obtained with the CCD camera in order to account for camera noise. This pixel-by-pixel operation is conveniently performed by Spyglass Transform® software.

The next step in the image-processing procedure is to build a TSP calibration curve. Experience has shown that *a priori* calibration does not provide the most accurate results, because TSP degrades over time, and experimental settings, such as lighting, are not exactly the same for every experiment. Therefore, TSP responses are different for virtually every new experimental condition. The most accurate results are obtained by performing *in-situ* calibration; that is, intensity data are obtained while an actual experiment is running and are directly correlated with a limited number of thermocouple temperature measurements to provide the calibration curve.

For *in-situ* calibration, the intensity values of a 3 × 3 pixel array centered around each thermocouple location were extracted from every ratioed image. Their average intensity from the images was then plotted against the thermocouple temperature measurement at the same location. This is done repeatedly until all the thermocouples, and all the images are processed. Typically, seven thermocouples were placed on the heated plate, giving seven calibration points for each experimental condition. Once a calibration curve is developed, the full-field surface temperature distributions of the TSP surfaces are obtained simply by converting intensity-based image data to temperature.

5. Results and discussion

5.1 Calibration surface

An *in-situ* calibration curve for the TSP surface is shown in Fig. 3. The intensity ratio, I_{ref}/I_{run}, of the TSP increases with temperature; in other words, the TSP intensity, I_{run}, decreases as temperature increases. Therefore, the TSP surface would be brightest at 0 K. Fitting the calibration curve in the form of Eq. (1) gives an activation energy of E_a/R = 2842 K. Note that this activation energy can vary for different experiments or different batches of TSP.

Figure 3 shows that the PUR TSP is sensitive throughout the range of temperatures tested from 24 to 50°C. Woodmansee (1997) also generated a PUR TSP calibration surface from 0 to 30°C. Thus, it can be concluded that PUR TSP is sensitive from 24 to 50°C. Moreover, it seems that it could be applied at even lower or higher temperatures. On the other hand, one of the restrictions for TSP to be applied over a wide range of temperatures is its binder, shellac, for

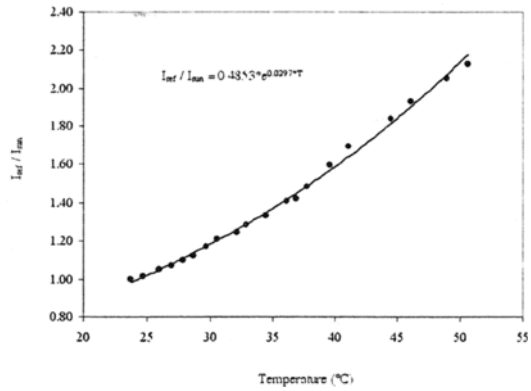

Fig. 3. TSP calibration curve from 24 to 50°C.

the case of PUR TSP. Shellac melts upon excessive heating or cracks upon excessive cooling. In summary, the recommended temperature range for PUR TSP is between 0 and 50°C.

Another strength of TSP is that it is fairly sensitive to a small temperature change. Based on the calibration curve in Fig. 3, 0.5°C change in temperature causes about 1.5% change in the TSP intensity ratio, which is easily detected by the CCD camera.

The maximum and minimum temperature differences between the thermocouple and TSP measurements are 1.01°C and 0.01°C, respectively, while the standard deviation of all the temperature differences is 0.26°C. Therefore, the TSP-predicted surface temperatures match the thermocouple measurements within 0.52°C with 95% confidence.

5.2 Flat plate heat transfer

As a first experimental application of TSP, Fig. 4 shows the surface temperature distribution of the flat plate under constant heat flux conditions. The continuous, two-dimensional nature of this surface reveals the strength of the TSP method. Such similar whole-surface temperature distributions cannot be obtained easily by traditional methods, such as thermocouple or RTD measurements. Moreover, the profiles are smooth and accurate because no intrusive measuring devices are used, which otherwise would block and/or alter the flow field.

The local Nusselt number (based on the constant heat flux condition) vs. local Reynolds number is plotted for the TSP measurements and the Blasius solution over the plate length in Fig. 5. In general, the TSP results match the analytical Blasius solution

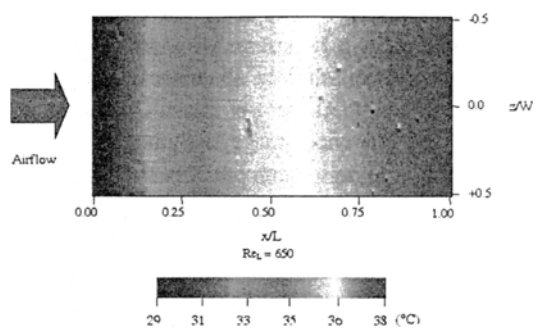

Fig. 4. Local temperature distribution for the flat plate, Re_L = 650, $q'' = 4.3$ W/m^2.

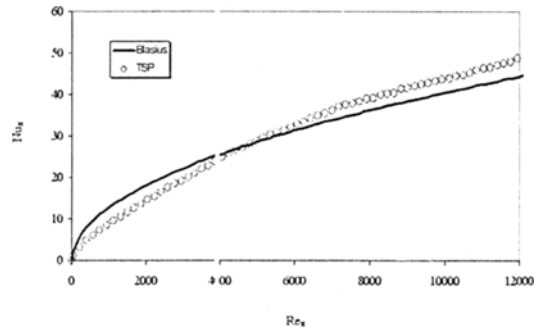

Fig. 5. Nu_x vs. Re_x for TSP measurements and Blasius solution.

relatively well. Near the leading edge the TSP results are somewhat below the Blasius solution. Further downstream, the TSP results then are slightly above the Blasius solution. However, this slight mismatch is mainly due to the experimental setup of the flat plate, not the TSP method itself. Factors such as leading edge effects and imperfect alignment between the flat plate and the freestream velocity vector could cause this mismatch. It has been also found that the voltage drop across the heater foil and, therefore, the heat flux, is not perfectly uniform; the voltage drop at the leading edge is about 6% higher than that at the trailing edge. This slightly non-uniform flux condition also contributes to the mismatch between the theoretical and experimental results.

5.3 Heat transfer enhancement by vortex generators

Vortex generators are commonly used for the purpose of enhancing heat transfer. When the flow encounters a vortex generator, an adverse pressure gradient causes the boundary layer to separate and form a swirling flow, or vortex, as shown in Fig. 6. A

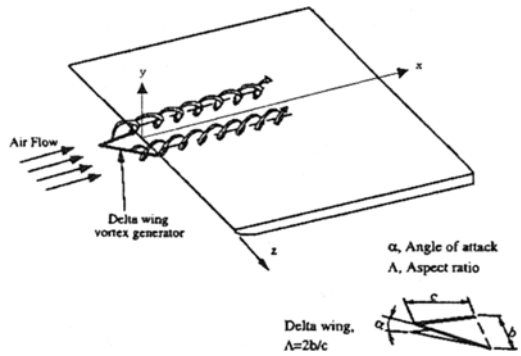

Fig. 6. Tip vortices generated by a delta wing. (modified from Gentry, 1998)

delta wing can generate such a vortex system that enhances the mixing of the fluid near the plate surface with the fluid from the freestream. Therefore, heat transfer is enhanced in this way as the temperature gradient increases at the surface (Gentry and Jacobi, 2002; Jacobi and Shah, 1998). Note that the difference between this work and that of Gentry and Jacobi (2002) is that they used naphthalene sublimation for the heat transfer measurements, which is a much more cumbersome technique than TSP, especially for the local results.

For delta wings, the aspect ratio, Λ and angle of attack are defined to be (2b/c) and α, respectively, as shown in Fig. 6. Delta wings with Λ = 1.25; α = 35 ° and Λ = 2.0; α = 35° have been tested in this experiment. Figures 7(a) and 7(b) show the TSP-measured surface temperature distribution on the flat plate downstream of the delta wing vortex generator. The path of the tip vortices is clearly observable, as the local temperatures are lower where the vortices have swept cooler freestream fluid onto the surface. From Fig. 7(b), it can be seen that the delta wing with a higher aspect ratio caused larger vortices that affected a wider area behind the vortex generator. In order to quantify the amount of heat transfer enhancement obtained with the delta wing, the ratio of the Nusselt number with the delta wing to the Nusselt number without the delta wing is plotted in Fig. 8(a) (three-pixel wide average column along spanwise centerline) and Fig. 8(b) (three-pixel wide average spanwise column at x/L = 0.3). Three columns and rows of pixels were averaged for the streamwise and spanwise Nusselt number distributions plotted. The maximum enhancement is about 30 % for the given geometry of the delta wing.

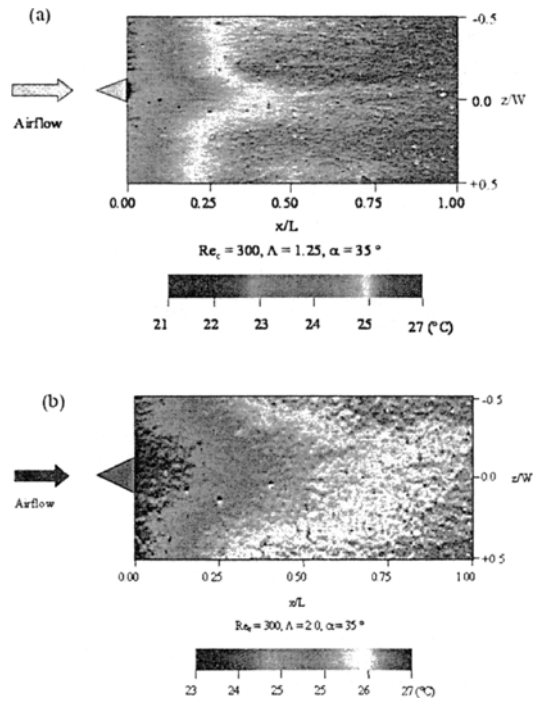

Fig. 7. Local temperature distribution for flat plate with delta wing.
(a) Λ = 1.25; α = 35 °; Re_c = 300, $q'' = 1.6$ W/m^2
(b) Λ = 2.0; α = 35 °; Re_c = 300, $q'' = 1.6$ W/m^2

A bit of asymmetry in the spanwise result may be due to the asymmetry of the delta wing and its attachment to the flat plate, and the fact that the flow path of the vortex system is not perfectly parallel to the centerline. From Fig. 8(a), it is interesting to note that less heat transfer occurs due to a blockage effect immediately behind the delta wing where the vortices have not touched the surface, as the boundary layer is lifted. On the other hand, the maximum enhancement occurs about one-third down the plate as the swirling vortices enhance the mixing of the freestream and boundary layer the most. From these example results, it is clear that an optimal vortex generator can be chosen by utilizing the TSP method. More importantly, the locations of extremes in surface temperature are easily determined from the full-field TSP temperature distributions. Therefore, it is clear that TSP is a powerful and valuable tool, as it provides not only the whole-field surface temperature distributions but also the locations of temperature extremes.

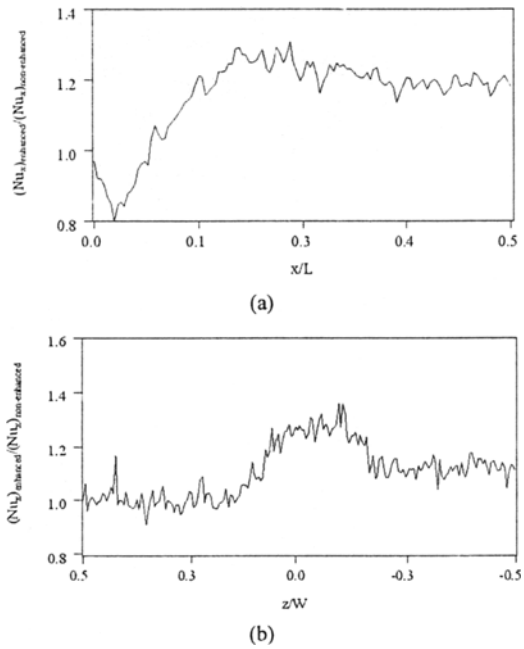

Fig. 8. Spanwise heat transfer enhancement by a delta wing.
(a) $\Lambda = 1.25$; $\alpha = 35$ °; $Re_c = 300$; $z/W = 0.0$
(b) $\Lambda = 1.25$; $\alpha = 35$ °; $Re_c = 300$; $x/L = 0.3$

5.4 Uncertainty analysis

The values of the deviations between the thermocouple and TSP measurements for all experiments (calibration, flat plate, and vortex generator) are summarized in Table 1. It can be seen that the TSP measurements match the thermocouple measurements within 0.5 to 0.8°C at 95% confidence (two standard deviations) for these experiments.

There are several sources of uncertainties involved in data acquisition and processing of the TSP images. The largest uncertainty comes from the attachment of the thermocouples to the heater foil surface. Since the foil is only 0.05 mm thick, it is difficult to bond the thermocouple bead securely on the foil surface. Also, the fact that the thermocouples are placed on the backside of the foil, not directly on the TSP surface itself, adds another uncertainty in the TSP calibration procedure. However, this uncertainty is unavoidable because mounting thermocouples directly on the painted surface is intrusive and makes it more difficult to determine intensity values around the thermocouples. Since the thermocouple itself is another measurement technique to obtain surface temperatures, some uncertainty is also associated with its reading, when the intensity data are matched to the thermocouple readings and voltage values are converted to temperatures.

Table 1. Absolute differences between thermocouple and TSP measurements for all experiments.

Temperature Difference (°C)	Calibration	Flat Plate	Vortex Generator
Mean	0.38	0.65	0.3
RMS	0.07	0.16	0.03
Standard Deviation	0.26	0.4	0.18
Maximum	1.01	1.33	0.86
Minimum	0.01	0.05	0.02

In addition, the TSP surface is a relatively thick coating that adds extra resistance to the heat transfer from the foil surface and thus changes the heat transfer coefficient for the flat plate heat transfer experiment. For the vortex generator experiment, some uncertainty is also involved with its aspect ratio, Λ, and angle of attack, α. However, the error (spatial smearing) due to this averaging is estimated to be less than 1%, since each pixel is only 0.3×0.3 mm^2 whereas the whole plate area is 154×154 mm^2. As discussed previously, the experimental setup and geometry are also sources of uncertainty involved in the experiments.

5.5 Signal noise reduction

Several techniques for reducing sources of signal noise have been introduced in this paper. First, acquiring ensembles of images (usually 20) of each experimental condition and averaging them greatly helps reduce the level of random noise (precision error). Second, normalization (described earlier) is a technique to reduce the effects of uneven lighting and variations in the TSP coating. Third, it is also helpful to mix a new batch of TSP and apply it to the surface just before imaging the TSP, because a fresher paint surface generates less noise. In addition, keeping the TSP surface clean and intact is another way to improve noisy images. Fourth, since the TSP method relies heavily on image processing and normalization, even a one- or two-pixel shift between the reference image and the run image results in large noise in the ratioed image. Therefore, maximum care is necessary so as not to move any equipment during the experiment. If pixel shift is unavoidable, as in high-speed flow experiments that have been done in the

past, image alignment routines can be employed during image processing as performed in Woodmansee (1997). Lastly, the quality of the TSP images also depends significantly on the quality of the image acquisition equipment. Therefore, scientific imaging devices, such as the CCD camera used in this work, are recommended.

6. Conclusion and recommendations

A number of heat transfer enhancement systems require measurement of whole-field surface temperature distributions in order to predict the points of temperature extremes, which might coincide with thermally and mechanically stressed points and could eventually result in failure. In this regard, temperature-sensitive paint is a valuable full-field method to determine the surface temperature distributions for various heat transfer enhancement applications in a non-intrusive way and at a relatively low cost.

TSP surface temperature distributions are determined from intensity variations of the luminescent coating. As a result of the TSP surface calibration work performed here, PUR TSP has been found to be applicable over at least the temperature range from 0 to 50°C. Applying TSP to a flat plate-vortex generator system to determine the surface temperature and local Nusselt number distributions was successful. The TSP Nusselt number distribution over the flat plate matches the Blasius solution with less than 10% error. For this experiment, a smooth, two-dimensional whole-field temperature distribution was obtained, which is not possible by traditional point measurement methods, such as thermocouple or RTD measurements. The TSP surface temperature measurements for the flat plate with the delta wing vortex generator also show local heat transfer enhancement and the locations of temperature extremes. The TSP method is quite attractive in that the intensity data of TSP are easy to obtain, process, and interpret, with the aid of high-resolution imaging tools and software.

There are also some limitations and improvements that can be made to the TSP method. For instance, TSP intensity variations are hardly visible with the bare eye. The TSP method requires relatively sophisticated experimental equipment to examine the effects of temperature variations. In addition, shellac, the binder of PUR TSP, is susceptible to relatively high or low temperatures. Using it for high-temperature applications, such as turbine blades, is not possible. It is also not well known which formulation of TSP is suitable for various temperature ranges. Therefore, further developments, such as searching for a more heat-resistant binder and exploring optimal probe molecule formulations, are recommended to make the TSP method more widely applicable. Since all the experiments in this paper have been done on flat surfaces, it would be worthwhile to apply TSP on curved surfaces to further investigate data acquisition and reduction issues for these experiments. Lastly, it would be valuable to compare the TSP method with other whole-field surface temperature measurement techniques, such as liquid crystal thermography.

Acknowledgments

The authors wish to thank Mark Woodmansee and Prashantha Bhat, who have been a significant help with the TSP method, the UIUC Air Conditioning and Refrigeration Center and its sponsors, and the National Science Foundation.

Nomenclature

α : Thermal diffusivity, [m^2/s] or angle of attack, [°]
Λ : Aspect ratio of delta wing, 2b/c, [-]
b : Width of delta wing, [m]
c : Chord length of delta wing, [m]
I_{ref} : Reference intensity
I_{dark} : Dark image intensity
I_{run} : Run image intensity
L : Plate length, [m]
Nu_x : Nusselt number based on downstream distance, [-]
q'' : Heat flux, q/A, [W/m^2]
Re_x : Reynolds number based on downstream distance, [-]
Re_c : Reynolds number based on chord length, [-]
Re_L : Reynolds number based on flat plate length, [-]
T : Temperature, [°C]
T_{ref} : Reference temperature, [°C]
x : Downstream distance from the leading edge of the flat plate, [m]
y : Vertical distance from the surface of the flat plate, [m]
z : Spanwise distance from the centerline of the flat plate, [m]

References

Campbell, B. T., Crafton, J., Witte, G. R. and Sullivan, J. P., 1998, "Laser Spot Heating/Temper-

ature-Sensitive Paint Heat Transfer Measurements," *20th AIAA Advanced Measurement and Ground Testing Technology Conference*, Albuquerque, NM, AIAA 98-2501.

De Jong, N. C. and Jacobi, A. M., 2003, "Heat Transfer and Pressure Drop for Flow Through Bounded Louvered-Fin Arrays," *Experimental Thermal and Fluid Science*, 27, 237~250.

Gentry, M. C., 1998, "Heat Transfer Enhancement Using Tip and Junction Vortices," Ph.D. Thesis, Department of Mechanical and Industrial Engineering, University of Illinois at Urbana-Champaign, Urbana, IL.

Gentry, M. C. and Jacobi, A. M., 2002, "Heat Transfer Enhancement by Delta Wing-Generated Tip Vortices in Flat Plate and Developing Channel Flows," *Journal of Heat Transfer*, 124, 1158~1168.

Jacobi, A. M. and Shah, R. K., 1998, "Air-Side Flow and Heat Transfer in Compact Heat Exchangers: A Discussion of Enhancement Mechanisms," *Heat Transfer Engineering*, 19:4, 29~41.

Liu, T. and Sullivan, J., 2004, "Pressure and Temperature Sensitive Paint," *Springer-Verlag*. Heidelberg, Germany.

Liu, T., Campbell, B. T., Burns, S. P. and Sullivan, J. P., 1997, "Temperature and Pressure-Sensitive Paints in Aerodynamics," *Applied Mechanics Review*, Vol. 50, pp. 227~246.

Woodmansee, M. A., 1997, "Temperature-Sensitivity Effects of Pressure-sensitive Paint and Associated Wind Tunnel Data Reduction Methods," M. S. Thesis, Department of Mechanical and Industrial Engineering, University of Illinois at Urbana-Champaign, Urbana, IL.